



Published in final edited form as:

Arthritis Rheumatol. 2014 April 1; 66(4): 990–999. doi:10.1002/art.38319.

CTLA4-Ig Induced T-Cell Anergy Promotes Wnt10b Production and Bone Formation

Susanne Roser-Page, MS¹, Tatyana Vikulina, DDS², Majd Zayzafoon, MD, PhD³, and M. Neale Weitzmann, PhD^{1,2,4}

¹Atlanta Department of Veterans Affairs Medical Center, Decatur, Georgia 30033, USA

²Division of Endocrinology and Metabolism and Lipids, Department of Medicine, Emory University School of Medicine, Atlanta, GA, 30322, USA

³Department of Pathology, University of Alabama at Birmingham, Birmingham, AL 35294, USA

⁴Emory Winship Cancer Institute, Emory University, Atlanta, GA, 30322, USA

Abstract

Objective—Rheumatoid arthritis (RA) is an inflammatory autoimmune disease characterized by severe joint erosion and systemic osteoporosis. Chronic T-cell activation is a hallmark of RA and agents that target the CD28 receptor on T-cells, needed for T-cell activation, are being increasingly employed as therapeutic agents in RA and other inflammatory diseases. Lymphocytes play complex roles in the regulation of the skeleton and although activated T-cells and B-cells secrete cytokines that promote skeletal decline, under physiological conditions lymphocytes also play key protective roles in the stabilization of skeletal mass. Consequently, disruption of T-cell costimulation may have unforeseen consequences on physiological bone turnover. In this study we investigate the impact of pharmacological CD28 T-cell costimulation blockade on physiological bone turnover and structure.

Methods—C57BL6 mice were treated with Cytotoxic T-lymphocyte-associated protein 4 (CTLA4)-Ig, a pharmacological CD28 antagonist, or irrelevant control antibody (Ig) and serum biochemical markers of bone turnover quantified by ELISA. Bone mineral density (BMD) and indices of bone structure were further quantified by dual energy X-ray absorptiometry (DEXA) and micro-computed tomography (μ CT) respectively and static and dynamic indices of bone formation quantified using bone histomorphometry.

Results—Pharmacological disruption of CD28 T-cell costimulation in mice, significantly increased bone mass and enhanced indices of bone structure, a consequence of enhanced bone formation, concurrent with enhanced secretion of the bone anabolic factor Wnt10b by T-cells.

Address correspondence to: M. Neale Weitzmann, Division of Endocrinology & Metabolism & Lipids, Emory University School of Medicine, 101 Woodruff Circle, 1305 WMB, Georgia 30322-0001. mweitzm@emory.edu.

AUTHOR CONTRIBUTIONS

All authors were involved in drafting the article or revising it critically for important intellectual content, and all authors approved the final version to be published. Dr. Weitzmann had full access to all of the data in the study and takes responsibility for the integrity of the data and the accuracy of the data analysis.

Study conception and design. Weitzmann.

Acquisition of data. Roser-Page, Vikulina, Zayzafoon.

Analysis and interpretation of data. Weitzmann, Zayzafoon.

Conclusion—Inhibition of CD28 co-stimulation by CTLA4-Ig promotes T-cell Wnt10b production and bone formation and may represent a novel anabolic strategy for increasing bone mass in osteoporotic conditions.

RA is a chronic inflammatory autoimmune disease that leads to bone loss around inflamed joints, as well as a generalized systemic osteoporosis (1–3). Lymphocytes play central roles not only in the initiation and progression of the inflammatory state, but also in the bone loss associated with RA (4–8). Lymphocytes drive bone turnover as a consequence of the immuno-skeletal interface, an enigmatic centralization of immune and skeletal functions around common cell types and cytokine effectors (9). Immune cells including T-cells, B-cells, and antigen presenting cells (APC) are implicated in the regulation of basal (10) and/or pathological bone turnover (11). Activated lymphocytes induce bone resorption by secreting Receptor activator of NF- κ B ligand (RANKL), the key osteoclastogenic cytokine, and inflammatory factors including TNF α , a key driver of inflammatory cascades in RA. In addition, activated T cells produce Secreted osteoclastogenic factor of activated T-cells (SOFAT), a RANKL-independent osteoclastogenic cytokine, that may contribute to bone loss in RA (12, 13) and in periodontal infection (14).

In contrast, under physiological conditions lymphocytes are protective of the skeleton, as both human (15) and rodent B-cells (9, 10) secrete the RANKL decoy receptor Osteoprotegerin (OPG). Because T-cell costimulatory interactions amplify B-cell OPG production (10, 15) disruptions to adaptive immune function can lead to RANKL/OPG imbalances permissive for osteoclastogenesis. Indeed, alterations to the immuno-skeletal interface causing a B-cell inversion in OPG and RANKL production may account, in part, for bone loss characteristic of HIV-infection (9, 16, 17).

T-cells express several unique receptors/ligands necessary for immune regulation including the CD28 receptor, that binds to CD80/CD86 ligands expressed by APCs and mediates signals necessary for T-cell activation following binding of the T-cell receptor (TCR) to antigen bearing MHC complexes. Failure to activate CD28, or inhibition of CD28 signaling by CTLA4, a physiological modulator homologous to CD28 that competes for its ligands, leads to abortive T-cell activation and/or terminates immune responses resulting in T-cell anergy or deletion (18, 19).

CTLA4-Ig (Abatacept), an anti-inflammatory pharmaceutical comprising the binding domain of human CTLA4 fused to human IgG1, is approved for treatment of refractory RA in adults (20) and for juvenile idiopathic arthritis in children (21).

Our group has reported that CTLA4-Ig mitigates ovariectomy-induced bone loss by reducing T-cell activation and expression of TNF α by disrupting communication between T-cells and dendritic cells (22). Similarly, CTLA4-Ig ameliorates bone loss in mice treated with continuous infusion of PTH, a model of hyperparathyroidism (23). Furthermore, CTLA4-Ig is reported to directly suppress osteoclast differentiation in the absence of T-cells *in vitro* and to inhibit inflammatory bone erosion *in vivo* in an animal model of RA (24).

Because CTLA4-Ig disrupts co-stimulatory interactions between B-cells and T-cells, it has the potential to not only lower immune activation responsible for driving inflammation, but

also to disrupt basal bone turnover by disturbing the immuno-skeletal interface and B-cell OPG production. This effect has the potential to offset the gains in bone mass associated with reduced inflammation.

In this study we investigated the net effect of CTLA4-Ig on basal bone turnover and mass in mice by quantifying indices of bone structure and turnover. CTLA4-Ig led to significant bone accrual but surprisingly as a consequence of increased bone formation, as a likely consequence of T-cell expression of the bone anabolic ligand Wnt10b. Our data show for the first time that CTLA4-Ig leads to induction of bone formation and may have potential applications as a novel bone anabolic agent.

MATERIALS AND METHODS

All reagents were purchased from the Sigma-Aldrich Chemical Co. (St. Louis, MO), unless otherwise indicated.

Mice

All animal studies were approved by both the Atlanta VAMC and Emory University Animal Care and Use Committees and were conducted in accordance with the NIH Laboratory Guide for the Care and Use of Laboratory Animals.

Mice were housed under specific pathogen free conditions and were fed gamma-irradiated 5V02 mouse chow (Purina Mills, St. Louis, MO), and autoclaved water ad libitum. The animal facility was kept at $23 \pm 1^\circ\text{C}$, with 50% relative humidity and a 12/12 light/dark cycle.

Young (6 weeks of age) female C57BL6 WT and OTI mice were from Jackson Labs (Bar Harbor, ME) and skeletally mature (5 month old) mice were from the National Institute on Aging (NIA) aged mouse colony at Charles River Laboratories (Wilmington, MA). WT mice were injected with 10 mg/Kg CTLA4-Ig (Orencia: Bristol-Myers Squibb) twice weekly intraperitoneally or with human IgG (Lampire Biological Laboratories, Pipersville, PA) for 3 or 6 months (26 weeks) as indicated. Skeletally mature mice comprised 8 Ig and 7 CTLA4-Ig mice/group while young mice treated for 3 months comprised 10 mice/group. Young mice treated for 6 months comprised 12 mice/group however, one extreme outlier in the CTLA4-Ig group with a final mean BV/TV of 0.12, falling 3 SD below the average and well below even the WT mean value of 2.07, was eliminated from the μCT and histomorphometry analysis. One bone used for histomorphometry was damaged during processing and had no quantifiable bone or cells.

Bone densitometry

BMD (g/cm^2) quantifications were performed in anesthetized mice by DEXA using a PIXImus 2 bone densitometer (GE Medical Systems). Total body DEXA was performed and region of interest boxes placed to quantify anatomical sites including lumbar spine, femur and tibia as previously described (25). The left and right femurs and left and right tibias were averaged for each mouse and the mean used for group calculations.

Micro-Computed Tomography

μ CT was performed in L3 vertebrae and femoral metaphysis ex vivo to assess trabecular bone microarchitecture using a μ CT40 scanner (Scanco Medical AG, Bruettisellen, Switzerland) calibrated weekly with a factory-supplied phantom. A total of 405 tomographic slices were taken at the L3 vertebra (total area of 2.4 mm) and 100 tomographic slices at the distal femoral metaphysis and trabecular bone segmented from the cortical shell for a total area of 0.6 mm beginning approximately 0.5 mm from the distal growth plate. Projection images were reconstructed using the auto-contour function for trabecular bone. Cortical bone was quantified at the femoral mid-diaphysis from 100 tomographic slices. Representative vertebral samples based on mean BV/TV were reconstructed in 3D to generate visual representations. Indices and units were standardized per published guidelines (26).

Quantitative Bone Histomorphometry

Bone histomorphometry was performed at the University of Alabama at Birmingham, Center for Metabolic Bone Disease-Histomorphometry and Molecular Analysis Core Laboratory on trichrome-stained plastic-embedded sections of calcein labeled femurs from Ig and CTLA4-Ig injected mice.

Biochemical indices of bone turnover

CTx, and osteocalcin were quantified in mice serum using RATlaps (CTx) and Rat-MID (osteocalcin) ELISAs (Immunodiagnostic Systems Inc. Fountain Hills AZ).

Wnt10b ELISA—Wnt10b protein was determined in 24 hr conditioned media from negatively immunomagnetically purified CD3 T-cells (Miltenyi Biotec. Auburn, CA) using a Wnt10b ELISA (USCN Life Science Inc., Wuhan, P.R. China).

Real-time RT-PCR—Total RNA was extracted from whole nucleated bone marrow, flushed from long bones and dissolved in Trizol Reagent. Real-time RT-PCR was performed on an ABI Prism 7000 instrument (Applied Biosystems, Foster City, CA) as previously described (10) using commercial (Applied Biosystems) master mix and primer sets and probes for murine Wnt10b (Mm00442104), OPG (Mm 001205928), RANKL (Mm 00441906) and β -actin (Mm 00607939). Changes were calculated using the 2^{-Ct} method (27) with normalization to β -actin.

T cell activation assays

Plates were coated overnight with activating anti-mouse CD3e (5 ug/ml) and/or anti-mouse CD28 (25ug/ml) antibodies in sterile PBS (eBioscience, San Diego CA). Splenic T-cells were isolated using a CD3 Pan T cell isolation kit (Miltenyi Biotec.) and 12 replicate wells plated at 2×10^7 cells/well in 24 well plates in 750 μ l of RPMI1640 + 5% FBS for 24 hours and then dissolved in Trizol for RNA isolation and real time RT-PCR for Wnt10b expression as described above.

APC Assays

APC assays were performed as described with modifications (28). Briefly, immunomagnetically purified (Miltenyi Biotech.) splenic CD11c dendritic cells were used as APC and plated in triplicate at 150,000 cells/well in complete RPMI1640+10% FBS and incubated for 4 h at 37°C with 1 μ M antigen (ovalbumin (Ova) peptide, (SIINFEKL) from Invivogen, San Diego, CA) followed by two washes in medium. CD8⁺ T-cells expressing a monoclonal Ova specific transgenic TCR were purified from spleens of OTI mice and 1 million T-cells incubated with Ova presenting APC \pm CTLA4-Ig for 24 hr. T-cells and dendritic cells were dissolved in Trizol for RNA isolation and real time RT-PCR for Wnt10b expression as described above.

Statistical Analysis

Statistical significance was determined using GraphPad InStat version 3.0 for Windows (GraphPad Software Inc. La Jolla, CA). Gaussian distribution was assessed using the Kolmogorov and Smirnov test. Simple comparisons were made using 2-tailed Students t test or Mann-Whitney for non-parametric data. Group comparisons were made using one-way ANOVA with Tukey-Kramer Post Hoc test. $P < 0.05$ was considered statistically significant. $P = N.S$ (not significant).

RESULTS

Treatment of mice with CTLA4-Ig leads to an elevation in BMD, and enhanced trabecular and cortical bone volume

In order to investigate the net effect of the immunosuppressant agent CTLA4-Ig on physiological basal bone modeling we injected CTLA4-Ig or irrelevant isotype control Ig into young female (6-week-old) C57BL6 mice. BMD was examined after 12 and 26 weeks by bone densitometry using DEXA. Although CTLA4-Ig administration failed to cause any significant change in BMD compared to control immunoglobulin (Ig) control at 3 months (Figure 1A), by 6 months of treatment CTLA4-Ig injected mice displayed a significant increase in total body BMD and increases at specific anatomical sites including femur and tibia (left and right femur or tibia for each mouse independently averaged) and lumbar spine (Figure 1B).

To assess the effect of chronic CTLA4-Ig treatment on the remodeling skeletons of adult mice we further treated 5-month-old mice with CTLA4-Ig or control (Ig) for six months. As with young mice total body BMD was significantly elevated as was BMD at femur, lumbar spine and tibia (Figure 1C).

To provide independent evaluations of cortical and cancellous bone we employed μ CT of lumbar vertebrae and femurs. Representative μ CT reconstructions of vertebral trabecular bone are shown for young skeletally immature mice (6 weeks of age) treated for 3 months (Figure 1A, lower panel), young mice treated for 6 months (Figure 1B, lower panel) and in skeletally mature (5 months of age) mice treated for 6 months (Figure 1C, lower panel).

Quantitative microarchitectural indices of trabecular bone structure were further computed for young mice receiving 3 and 6 months of CTLA4-Ig treatment (Table I) and for mature mice receiving 6 months of treatment (Table II). Vertebral trabecular bone volume fraction (BV/TV) was significantly increased in young mice receiving CTLA4-Ig for both 3 and 6 months consistent with a decline in trabecular separation (Tb. Sp.), reflecting the amount of bone free space. Trabecular thickness (Tb. Th.) and trabecular number (Tb. N.) were significantly increased in young mice by 6 months of treatment but fell just short of significance at 3 months, suggesting a slow accumulation of bone volume over time. As expected bone accretion in mature mice was slower than in younger animals and BV/TV fell just short of statistical significance although Tb. N. and Tb. Sp., were significantly different to Ig treated controls.

Femoral trabecular BV/TV was significantly increased at both 3 and 6 months of treatment in young animals although changes in Tb. Sp., Tb. Th., and Tb. N. did not achieve statistical significance. In both cases Tb. Th., showed the largest increases and just narrowly fell short of significance at 6 months of treatment. These data suggest that CTLA4-Ig may work predominantly by expanding the thickness of preexisting trabecular spicules rather than catalyzing de novo synthesis of new template. Consistent with the age of the mature mice (11 months), there was very little trabecular bone remaining in the femurs. Despite inconsistency in the structural indices a large mean increase in BV/TV was quantified with CTLA4-Ig treatment. However, due to high variability within the groups, no statistically significant changes were achieved.

Cortical bone was quantified in the mid-femoral diaphysis and revealed a significant increase in cortical thickness (Co. Th.) in young mice (Table I) by 6 months while Cortical area (Co. Ar.) was increased in magnitude by 6 months but fell just short of statistical significance. Neither index reached statistical significance in mature mice. Because total body and all anatomical analyses of BMD by DEXA (Figure 1A) revealed significant increases in BMD in mature animals the data suggest that small increases in cortical bone across large areas may account for the increases resolved by DEXA but not by μ CT.

CTLA4-Ig enhances biochemical indices of bone formation but not indices of bone resorption in vivo

To assess the rates of bone resorption and bone formation in vivo bone turnover markers were quantified in the serum of CTLA4-Ig and Ig treated mice. Serum C-terminal telopeptide of collagen (CTx), a sensitive and specific index of bone resorption was not significantly changed between Ig and CTLA4-Ig treated groups in either young or mature mice and irrespective of time on treatment (CTx: Young mice 6 months (Ig: 24.7 ± 5.7 vs. CTLA4-Ig; 23.8 ± 9.4) and mature mice 6 months (Ig: 13.2 ± 5.9 vs. CTLA4-Ig 14.2 ± 3.3). Mean \pm SD, P=N.S.

Consistent with these data RT-PCR of total bone marrow revealed no significant alterations in expression of OPG and RANKL at 26 weeks (2^{-CT} of OPG: Ig (1.00 ± 0.18) vs. CTLA4-Ig (0.87 ± 0.17), and 2^{-CT} of RANKL: Ig (1.00 ± 0.04) vs. CTLA4-Ig (0.88 ± 0.05); mean \pm SD, P=NS).

By contrast, serum osteocalcin, a biochemical marker of in vivo bone formation was dramatically increased in young mice treated with CTLA4-Ig for 3 months, 6 months and in mature mice treated for 6 months (Figure 2A). These data suggest that bone accretion was a consequence of elevated bone formation.

CTLA4-Ig enhances indices of bone formation quantified by bone histomorphometry

As osteocalcin reflects global bone formation across all bone surfaces we further employed quantitative bone histomorphometry to assess bone formation in young mice treated for 6 months with CTLA4-Ig at a tissue and cellular level. Three indices of bone formation mineralizing surface (MS), mineral apposition rate (MAR) and bone formation rate (BFR) normalized for TV (BFR/TV) were all significantly increased (Table III). When MS and BFR were normalized for bone surface (BS) BFR fell just short of significance while BFR and MS normalized for BV were unchanged from control. The static indices, osteoblast surface (Obs)/BS and number of osteoblasts (N.Ob)/BS, showed a non-significant decline indicating that the long term effect of CTLA4-Ig was not to increase osteoblast number, but rather induce activation of pre-existing osteoblasts driving a wave of new bone formation. As a consequence, the number of osteoblasts and the area of bone covered by osteoblasts both appeared to decline as a result of the significantly increased bone surfaces. BFR/TV, which normalizes for total bone area is the index that correlates most closely with bone turnover markers such as osteocalcin (29). Similarly, small non-significant declines in osteoclast number (N.Oc/BS) and surface (OcS/BS) were observed, and likely also reflect the relative increase in BS, rather than long term direct effect of CTLA4-Ig on osteoclast number. Cancellous structural indices including BV, BV/TV, Tb. N. and Tb. Sp. as computed by histomorphometry all showed robust changes supporting gain of bone mass as observed in the μ CT data. Surprisingly, the percentage change in BV/TV of femoral bone determined by histomorphometry was more than twice that observed by μ CT. In principle μ CT is a more robust and reliable measure of bone volume and structure than histomorphometry as μ CT reflects a true 3D quantification of a relatively large segment of bone while histomorphometry is a 2D representation of a comparatively small number of slices. This diminished precision likely accounts for the apparent discrepancy.

Representative double calcein labels from which MAR and BFR indices were calculated are shown in Figure 2B and reveal enhanced bone formation in young CTLA4-Ig treated animals at 6 months of treatment. Representative photomicroscopy images of Goldner Trichrome stained femoral sections are shown in Figure 2C and show enhanced numbers of trabecular elements in the femoral metaphysis (yellow arrows) and increased bone thickness in the epiphyses above the growth plate (red arrows).

The anabolic Wnt ligand, Wnt10b is significantly elevated in total bone marrow and purified T-cells from CTLA4-Ig treated mice

T-cells have the capacity to secrete Wnt10b, a potent bone anabolic Wnt ligand (30). As a possible explanation for the anabolic activity of CTLA4-Ig we quantified Wnt10b expression by CTLA4-Ig and Ig treated mice in the bone marrow using real time RT-PCR and in conditioned medium from purified CD3⁺ T-cells by ELISA (Figure 3A). Wnt10b expression was found to be significantly elevated in the bone marrow of CTLA4-Ig treated

animals and protein production by purified CD3⁺ T-cells, suggesting involvement of Wnt10b by T-cells in the anabolic activity of CTLA4-Ig.

CD28 inhibits Wnt10b expression by activated T-cells in vitro, while CTLA4-Ig-suppression of CD28 signaling amplifies Wnt10b expression induced by Antigen Presentation in vitro

To further explore the mechanism of T-cell Wnt10b production by CTLA4-Ig we purified T-cells and activated them in vitro using CD3e activating antibody in the presence or absence of activating CD28 antibody. Activation of CD3 led to a significant upregulation of Wnt10b expression at 24 hr (Figure 3B). Activation of CD28 alone had no significant effect on Wnt10b but potently inhibited Wnt10b expression induced by CD3. CTLA4-Ig may thus promote Wnt10b expression in T-cells by blocking the interaction of CD80/CD86 on APC with T-cell expressed CD28, a negative signal for Wnt10b expression. To test this hypothesis directly we performed an in vitro APC assay in which purified dendritic cells were used as APC to express Ova antigen to CD8⁺ T-cells expressing a monoclonal TCR with Ova-specific recognition. Presentation of Ova by APC to T cells led to induction of Wnt10b expression that was potently super-induced by addition of CTLA4-Ig to the culture (Figure 3C).

DISCUSSION

Our data demonstrate for the first time that pharmacological suppression of CD28 costimulation by CTLA4-Ig results in a bone anabolic signal, a likely consequence of T-cell Wnt10b secretion.

Although the capacity of the immune system to regulate bone resorption through perturbations of the immunoskeletal interface is well studied, little is known regarding the ability of the immune system to regulate bone formation. Activated T-cells have been previously reported to secrete cocktails of cytokines that cumulatively have the capacity to induce alkaline phosphatase activity in purified human bone marrow stromal cells and elevate expression of Runx2 and osteocalcin mRNA (31). By contrast a number of cytokines involved in immune regulation such as IL-7 (32) or produced by immune cells including T-cells and macrophages, such as TNF α (33), may act to uncouple bone formation from resorption under inflammatory conditions. Thus, by suppressing the natural compensatory increase in bone formation in response to increased bone resorption bone homeostasis is disrupted leading to bone loss (11, 32).

Indeed, CTLA4-Ig has been reported to ameliorate short-term ovariectomy-induced bone loss by reducing T-cell activation and inflammatory cascades (22) and to directly suppress osteoclast differentiation *in vitro* and inflammatory bone erosion *in vivo* in an animal model of TNF α -induced arthritis (24).

Understanding the molecular mechanism by which CTLA4-Ig stimulates Wnt10b production remains to be studied in detail. However, based on our data and published studies we propose a model whereby Wnt10b production is an unintended consequence of abortive T-cell activation due to disruption of the dual-signal mechanism of T-cell activation. It is now established that two signals are required for full T-cell activation. The first signal is

generated when the TCR engages MHC class I or II bearing antigens on the surface of professional APC (B-cells, macrophages and dendritic cells). This first signal is insufficient for T-cell activation and on its own simply renders T-cells unresponsive to further antigenic stimuli (anergy) (18). At the molecular level this signal involves activation of the cAMP second messenger system. The generation of cAMP leads to activation of protein kinase A (PKA) and cAMP response element (CRE) binding (CREB) protein, a transcription factor that transactivates genes involved in T-cell regulation and anergy. This costimulatory signal involves binding of the CD28 receptor on T-cells, with B7 molecules (B7-1 (CD80) and B7-2 (CD86)), expressed on professional APC (including B-cells, macrophages and dendritic cells). Activation of CD28 leads to induction of phosphodiesterase, an enzyme that cleaves cAMP, neutralizing its second messenger activity and eliminating the repressive first signal, thus preventing anergy and allowing full T-cell activation to proceed (34). These two signals lead to full T-cell activation, cytokine production, clonal expansion, and prevention of anergy (18). In the context of normal *bona fide* immunological actions cAMP generation would be short lived as the “verification signal” transduced through CD28 would rapidly shut off this pathway, preventing release of Wnt10b. However, in the context of an impeded CD28 signal T-cell cAMP production would remain active leading to Wnt10b secretion and binding to Wnt receptors (LRP5 and 6) on osteoblasts leading to their activation and new bone formation. This model is presented diagrammatically in Figure 3D and is further supported by published gene array data demonstrating that Wnt10b expression is upregulated in anergic T-cells (38).

Interestingly, our group has previously reported that the anabolic activity of intermittent parathyroid hormone (PTH) is mediated in part through T-cell production of Wnt10b (30, 35), a Wnt ligand previously reported to be secreted by T-cells (36, 37). Because PTH is a potent inducer of cAMP we hypothesize that Wnt10b expression may be directly promoted by activation of cAMP in T-cells bypassing normal TCR mediated interactions with APC (TCR and CD28 signaling) leading to a potent sustained production of Wnt10b.

An interesting conundrum that is explained by this hypothesis is the question of why the genetic deletion of T-cells leads to an increase in bone resorption (10, 39, 40) but fails to dramatically curtail bone formation (30) while CD28 inhibition alone, induces bone formation. We speculate that Wnt10b production is only elicited in contexts involving a significant impediment to CD28 signaling (such as exogenous application of CTLA4-Ig or intermittent administration of PTH). Consequently, under physiological conditions basal T-cell activation is relatively weak and hence little Wnt10b is secreted. Even in inflammatory conditions CD28 activation during true APC-mediated T-cell activation would quickly silence Wnt10b expression.

Our group has reported that CTLA4-Ig is protective of ovariectomy and continuous PTH-induced bone loss by blunting osteoclastic bone resorption driven by inflammatory cytokines such as RANKL and TNF secreted by T cells. Anabolic effects were not observed in these relatively short studies and in fact our current data suggest that the anabolic effect of CTLA4-Ig is gradual but progressive, thus achieving significant bone gains over an extended period of time. Although, early changes in resorption may also occur following

CTLA4-Ig administration, our data suggest that the major net effect of chronic exposure, as used therapeutically in humans, is likely to be predominantly anabolic.

Consistent with high basal bone turnover in young mice rates of bone formation and bone accretion were robust in young mice treated with CTLA4-Ig. By contrast, bone accretion in skeletally mature mice was more modest and although we observed a strong trend towards bone gain, BV/TV in the vertebrae fell just short of statistical significance although some structural indices including Tb. N. and Tb. Sp were significantly changed. Femoral indices were not significantly increased, likely due to the rapid degradation of trabecular bone in the femurs of mice following peak BMD leaving a denuded template for osteoblasts to act on. Interestingly, although basal bone formation represented by serum osteocalcin was significantly diminished compared to younger mice, CTLA4-Ig did potentially promote bone formation in these mice suggesting that an anabolic response was in fact underway and that a statistically significant response would be likely given additional time.

The capacity of CTLA4-Ig to promoted bone formation in humans remains to be demonstrated, however administration of CTLA4-Ig to treat inflammatory diseases such as RA, may have multiple beneficial effects including reduced inflammation and reduced osteoclastic bone resorption driven by inflammation (22) as well as due to direct inhibitory effects on osteoclasts (24). The present study further suggests bone anabolic activities due to T-cell release of Wnt10b may further promote a beneficial balance between bone formation and resorption.

Contrary to inflammatory contexts our studies of basal bone turnover did not detect significant declines in CTx, an index of bone resorption, following chronic treatment with CTLA4-Ig. This was unexpected given that CTLA4-Ig is reported to mediate a direct anti-osteoclastic activity *in vitro* (24). A possible explanation is that early acute effects on osteoclasts are indeed observed early in the treatment but return to baseline over time.

In conclusion we show that CTLA4-Ig, a CD28 co-stimulation inhibitor, is a potent bone anabolic agent and promotes the production of Wnt10b by T-cells. While there are numerous antiresorptive drugs currently available the treatment of osteoporotic conditions, anabolic agents are few and far between. Currently, Teriparatide, a fragment of PTH administered intermittently is the only FDA approved modality for stimulating bone accretion. Abatacept may represent a novel anabolic agent that may be potentially repurposed to ameliorate osteoporosis by stimulating bone formation, either as a stand-alone agent or in combination with other anabolic or anti-catabolic agents.

Acknowledgments

This work was supported by a grant from the Biomedical Laboratory Research & Development Service of the VA Office of Research and Development (5I01BX000105). MNW was also supported, in part, by NIAMS grants (AR053607, AR056090 and AR059364) and NIA grant AG040013. The contents of this manuscript do not represent the views of the Department of Veterans Affairs or the United States Government.

Histomorphometry services were performed by the University of Alabama at Birmingham, Center for Metabolic Bone Disease-Histomorphometry and Molecular Analysis Core Laboratory, supported by NIAMS (P30AR46031).

References

1. Deodhar AA, Woolf AD. Bone mass measurement and bone metabolism in rheumatoid arthritis: a review. *Br J Rheumatol*. 1996; 35(4):309–22. [PubMed: 8624634]
2. Dequeker J, Maenaut K, Verwilghen J, Westhovens R. Osteoporosis in rheumatoid arthritis. *Clin Exp Rheumatol*. 1995; 13 (Suppl 12):S21–6. [PubMed: 8846540]
3. Gough AK, Peel NF, Eastell R, Holder RL, Lilley J, Emery P. Excretion of pyridinium crosslinks correlates with disease activity and appendicular bone loss in early rheumatoid arthritis. *Ann Rheum Dis*. 1994; 53(1):14–7. [PubMed: 8311548]
4. Fournier C. Where do T cells stand in rheumatoid arthritis? *Joint Bone Spine*. 2005; 72(6):527–32. [PubMed: 16087382]
5. Kong YY, Feige U, Sarosi I, Bolon B, Tafuri A, Morony S, et al. Activated T cells regulate bone loss and joint destruction in adjuvant arthritis through osteoprotegerin ligand. *Nature*. 1999; 402(6759):304–9. [PubMed: 10580503]
6. Edwards JC, Szczepanski L, Szechinski J, Filipowicz-Sosnowska A, Emery P, Close DR, et al. Efficacy of B-cell-targeted therapy with rituximab in patients with rheumatoid arthritis. *N Engl J Med*. 2004; 350(25):2572–81. [PubMed: 15201414]
7. He X, Kang AH, Stuart JM. Anti-Human type II collagen CD19+ B cells are present in patients with rheumatoid arthritis and healthy individuals. *J Rheumatol*. 2001; 28(10):2168–75. [PubMed: 11669151]
8. Yanaba K, Hamaguchi Y, Venturi GM, Steeber DA, St Clair EW, Tedder TF. B cell depletion delays collagen-induced arthritis in mice: arthritis induction requires synergy between humoral and cell-mediated immunity. *J Immunol*. 2007; 179(2):1369–80. [PubMed: 17617630]
9. Vikulina T, Fan X, Yamaguchi M, Roser-Page S, Zayzafoon M, Guidot DM, et al. Alterations in the immuno-skeletal interface drive bone destruction in HIV-1 transgenic rats. *Proc Natl Acad Sci U S A*. 2010; 107(31):13848–53. [PubMed: 20643942]
10. Li Y, Toraldo G, Li A, Yang X, Zhang H, Qian WP, et al. B cells and T cells are critical for the preservation of bone homeostasis and attainment of peak bone mass in vivo. *Blood*. 2007; 109(9):3839–48. [PubMed: 17202317]
11. Weitzmann MN, Pacifici R. Estrogen deficiency and bone loss: an inflammatory tale. *J Clin Invest*. 2006; 116(5):1186–94. [PubMed: 16670759]
12. Rifas L, Weitzmann MN. A novel T cell cytokine, secreted osteoclastogenic factor of activated T cells, induces osteoclast formation in a RANKL-independent manner. *Arthritis Rheum*. 2009; 60(11):3324–35. [PubMed: 19877052]
13. Weitzmann MN, Cenci S, Rifas L, Haug J, Dipersio J, Pacifici R. T cell activation induces human osteoclast formation via receptor activator of nuclear factor kappaB ligand-dependent and -independent mechanisms. *J Bone Miner Res*. 2001; 16(2):328–37. [PubMed: 11204433]
14. Jarry CR, Duarte PM, Freitas FF, de Macedo CG, Clemente-Napimoga JT, Saba-Chujfi E, et al. Secreted osteoclastogenic factor of activated T cells (SOFAT), a novel osteoclast activator, in chronic periodontitis. *Human immunology*. 2013; 74(7):861–6. [PubMed: 23619471]
15. Yun TJ, Chaudhary PM, Shu GL, Frazer JK, Ewings MK, Schwartz SM, et al. OPG/FDCR-1, a TNF receptor family member, is expressed in lymphoid cells and is up-regulated by ligating CD40. *J Immunol*. 1998; 161(11):6113–21. [PubMed: 9834095]
16. Ofotokun I, Weitzmann MN. HIV-1 infection and antiretroviral therapies: risk factors for osteoporosis and bone fracture. *Curr Opin Endocrinol Diabetes Obes*. 2010; 17(6):523–9. [PubMed: 20844427]
17. Ofotokun I, Weitzmann MN. HIV and bone metabolism. *Discov Med*. 2011; 11(60):385–93. [PubMed: 21616037]
18. Sayegh MH. Finally, CTLA4Ig graduates to the clinic. *J Clin Invest*. 1999; 103(9):1223–5. [PubMed: 10225963]
19. Najafian N, Sayegh MH. CTLA4-Ig: a novel immunosuppressive agent. Expert opinion on investigational drugs. 2000; 9(9):2147–57. [PubMed: 11060799]
20. Vital EM, Emery P. Abatacept in the treatment of rheumatoid arthritis. Therapeutics and clinical risk management. 2006; 2(4):365–75. [PubMed: 18360649]

21. Ilowite NT. Update on biologics in juvenile idiopathic arthritis. *Curr Opin Rheumatol*. 2008; 20(5): 613–8. [PubMed: 18698187]
22. Grassi F, Tell G, Robbie-Ryan M, Gao Y, Terauchi M, Yang X, et al. Oxidative stress causes bone loss in estrogen-deficient mice through enhanced bone marrow dendritic cell activation. *Proc Natl Acad Sci U S A*. 2007; 104(38):15087–92. [PubMed: 17848519]
23. Bedi B, Li JY, Grassi F, Tawfeek H, Weitzmann MN, Pacifici R. Inhibition of antigen presentation and T cell costimulation blocks PTH-induced bone loss. *Ann N Y Acad Sci*. 2010; 1192(1):215–21. [PubMed: 20392239]
24. Axmann R, Herman S, Zaiss M, Franz S, Polzer K, Zwerina J, et al. CTLA-4 directly inhibits osteoclast formation. *Ann Rheum Dis*. 2008; 67(11):1603–9. [PubMed: 18203760]
25. Toraldo G, Roggia C, Qian WP, Pacifici R, Weitzmann MN. IL-7 induces bone loss in vivo by induction of receptor activator of nuclear factor kappa B ligand and tumor necrosis factor alpha from T cells. *Proc Natl Acad Sci U S A*. 2003; 100(1):125–30. [PubMed: 12490655]
26. Bouxsein ML, Boyd SK, Christiansen BA, Guldberg RE, Jepsen KJ, Muller R. Guidelines for assessment of bone microstructure in rodents using micro-computed tomography. *J Bone Miner Res*. 2010; 25(7):1468–86. [PubMed: 20533309]
27. Livak KJ, Schmittgen TD. Analysis of relative gene expression data using real-time quantitative PCR and the 2^{(-Delta Delta C(T))} Method. *Methods*. 2001; 25(4):402–8. [PubMed: 11846609]
28. Kamphorst AO, Guermonprez P, Dudziak D, Nussenzweig MC. Route of antigen uptake differentially impacts presentation by dendritic cells and activated monocytes. *J Immunol*. 2010; 185(6):3426–35. [PubMed: 20729332]
29. Parfitt AM, Drezner MK, Glorieux FH, Kanis JA, Malluche H, Meunier PJ, et al. Bone histomorphometry: standardization of nomenclature, symbols, and units. Report of the ASBMR Histomorphometry Nomenclature Committee. *J Bone Miner Res*. 1987; 2(6):595–610. [PubMed: 3455637]
30. Terauchi M, Li JY, Bedi B, Baek KH, Tawfeek H, Galley S, et al. T lymphocytes amplify the anabolic activity of parathyroid hormone through Wnt10b signaling. *Cell Metab*. 2009; 10(3):229–40. [PubMed: 19723499]
31. Michelangeli F, Cordier M, Melandri P, Gaspaillard M, Migliori G, Maestraci P. Study of pressor drops during continuous peridural analgesia in gerontologic surgery. *Ann Anesthesiol Fr*. 1975; 16(6):429–36. [PubMed: 2059]
32. Weitzmann MN, Roggia C, Toraldo G, Weitzmann L, Pacifici R. Increased production of IL-7 uncouples bone formation from bone resorption during estrogen deficiency. *J Clin Invest*. 2002; 110(11):1643–50. [PubMed: 12464669]
33. Cenci S, Weitzmann MN, Roggia C, Namba N, Novack D, Woodring J, et al. Estrogen deficiency induces bone loss by enhancing T-cell production of TNF-alpha. *J Clin Invest*. 2000; 106(10): 1229–37. [PubMed: 11086024]
34. Bjorgo E, Solheim SA, Abrahamsen H, Baillie GS, Brown KM, Berge T, et al. Cross talk between phosphatidylinositol 3-kinase and cyclic AMP (cAMP)-protein kinase signaling pathways at the level of a protein kinase B/beta-arrestin/cAMP phosphodiesterase 4 complex. *Mol Cell Biol*. 2010; 30(7):1660–72. [PubMed: 20086095]
35. Bedi B, Li JY, Tawfeek H, Baek KH, Adams J, Vangara SS, et al. Silencing of parathyroid hormone (PTH) receptor 1 in T cells blunts the bone anabolic activity of PTH. *Proc Natl Acad Sci U S A*. 2012; 109(12):E725–33. [PubMed: 22393015]
36. Hardiman G, Kastelein RA, Bazan JF. Isolation, characterization and chromosomal localization of human WNT10B. *Cytogenetics and cell genetics*. 1997; 77(3–4):278–82. [PubMed: 9284937]
37. Ouji Y, Yoshikawa M, Shiroy A, Ishizaka S. Wnt-10b secreted from lymphocytes promotes differentiation of skin epithelial cells. *Biochem Biophys Res Commun*. 2006; 342(4):1063–9. [PubMed: 16510119]
38. Zha Y, Marks R, Ho AW, Peterson AC, Janardhan S, Brown I, et al. T cell anergy is reversed by active Ras and is regulated by diacylglycerol kinase-alpha. *Nat Immunol*. 2006; 7(11):1166–73. [PubMed: 17028589]
39. Gyarmati J Jr, Mandi B, Facht J, Varga S, Sikula J. Alterations of the connective tissue in nude mice. *Thymus*. 1983; 5(5–6):383–92. [PubMed: 6659024]

40. Lee SK, Kadono Y, Okada F, Jacquin C, Koczon-Jaremko B, Gronowicz G, et al. T Lymphocyte Deficient Mice Lose Trabecular Bone Mass With Ovariectomy. *J Bone Miner Res.* 2006

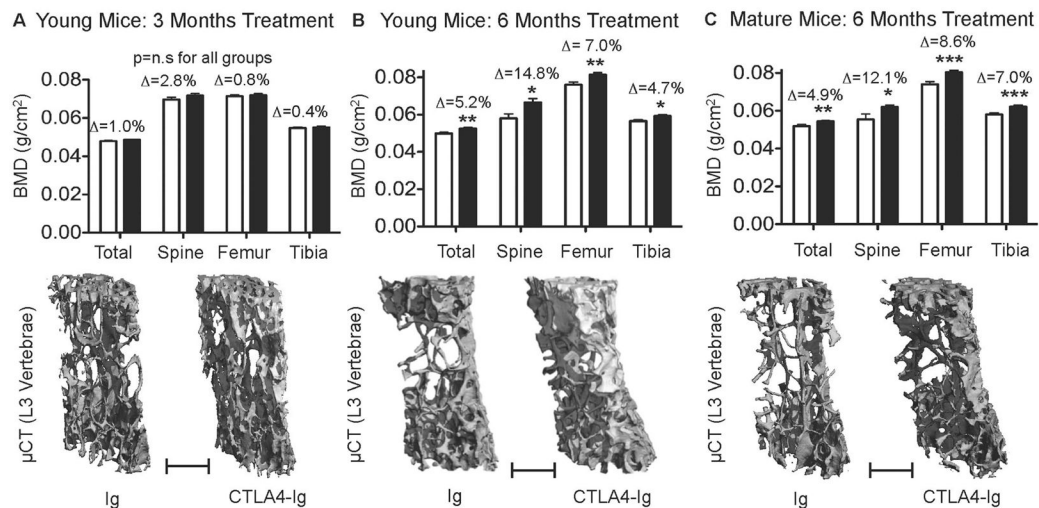


Figure 1. CTLA4-Ig promotes accretion of BMD and bone mass in young and skeletally mature mice

Total body BMD (Total) and BMD at lumbar spine (Spine), femur and tibia were quantified by DEXA in young mice: **A**, 3 and **B**, 6 months, after administration of Ig (control) or CTLA4-Ig and in: **C**, skeletally mature mice 6 months after CTLA4-Ig administration. Graphical data are presented as mean \pm SEM. Δ = percentage change from Ig. * $P < 0.05$; ** $P < 0.01$, *** $P < 0.001$. $p = n.s.$ (not significant). Young Mice 3 months treatment $n = 10$ mice/group; Young mice treated for 6 months, $n = 11$ and 12 for Ig and CTLA4-Ig respectively. Mature mice $n = 15$ mice/group. Representative high-resolution ($6 \mu\text{m}$) μCT reconstructions of vertebral cancellous bone for CTLA4-Ig or Ig are presented below the DEXA for each group. Scale Bar = $500 \mu\text{m}$.

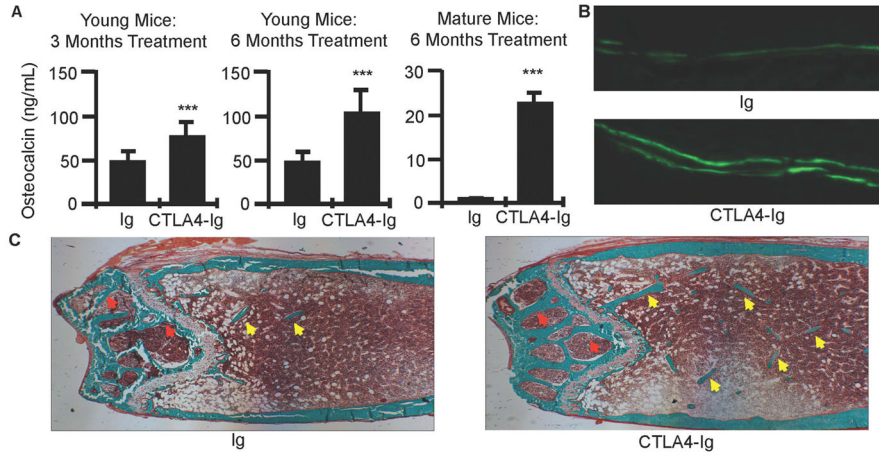


Figure 2. CTLA4-Ig promotes bone formation in mice

A, Serum markers of bone formation (osteocalcin) in young and skeletally mature mice treated with CTLA4-Ig or Ig for 3 and/or 6 months. Graphical data are presented as mean \pm SD. *** $P < 0.001$. **B**, Representative calcein double fluorescent labels in femurs from young mice treated for 6 months with CTLA4-Ig or Ig, used to compute mineral apposition and bone formation rates (40X mag.). **C**, Representative histological sections of Goldner's trichrome stained distal femur in young mice treated for 6 months with CTLA4-Ig or Ig. Mineralized bone stains green. Trabecular bone in bone marrow cavity indicated by yellow arrows and epiphyseal bone by red arrows. (100X mag).

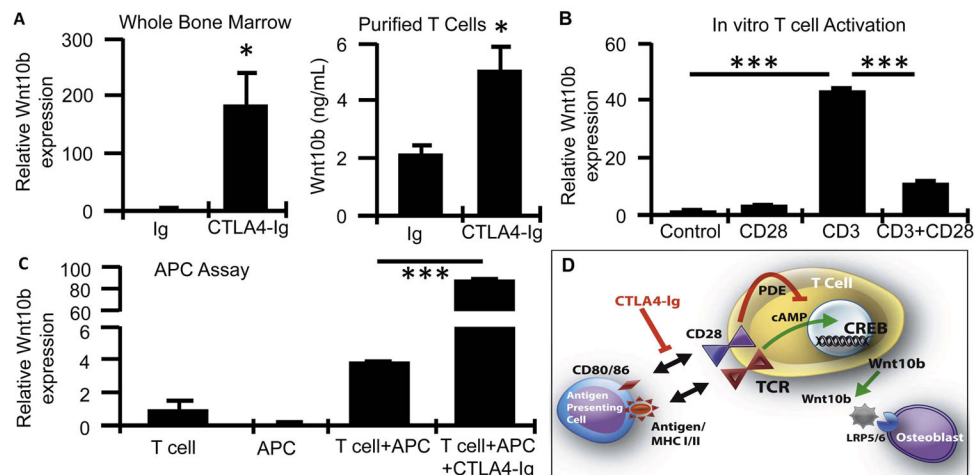


Figure 3. The bone anabolic Wnt ligand, Wnt10b is potently upregulated by CTLA4-Ig in vivo and suppressed by CD28 activation in vitro

A, Wnt10b production in Ig and CTLA4-Ig treated mice was quantified in whole bone marrow by real time RT-PCR and in conditioned media from purified T cells by ELISA. N= 4 mice/group, Mean \pm SEM. *P<0.05. **B**, Wnt10b expression quantified by RT-PCR in purified T cells activated by CD3 antibody with and without CD28 activating antibody. Mean \pm SD of 12 individual wells/group and representative of 2 independent experiments. **C**, Wnt10b quantified by RT-PCR in T cells activated in vitro by antigen presenting cells (APC) +/- CTLA4-Ig. Mean \pm SD of 3 individual wells/group and representative of 2 independent experiments. ***P<0.001. **D**, Model for anabolic response of CTLA4-Ig involving Wnt10b expression by T cells.

Table 1
 μ CT Indices from L3 Vertebrae of Young Mice administered Ig or CTLA4-Ig for 3 or 6 months

3 Months	Indices	Ig	CTLA4-Ig	% Change	P
L3 Vertebrae	BV/TV [%]:	13.15 ± 1.25	15.07 ± 0.95	+14.6	*0.0011
	Tb.Th. [mm]:	0.0390 ± 0.0010	0.0406 ± 0.0024	+4.0	0.0761
	Tb.N. [/mm]:	3.71 ± 0.20	3.91 ± 0.24	+5.4	0.0566
	Tb. Sp. [mm]:	0.2675 ± 0.0147	0.2526 ± 0.0161	-5.6	*0.0439
Femur	BV/TV [%]:	6.35 ± 1.35	8.04 ± 1.22	+18.8	*0.0088
	Tb.Th. [mm]:	0.0412 ± 0.0026	0.0433 ± 0.0037	+4.9	0.1490
	Tb.N. [/mm]:	3.44 ± 0.34	3.69 ± 0.32	-0.4	0.1091
	Tb. Sp. [mm]:	0.2822 ± 0.0147	0.2713 ± 0.0247	+2.0	0.2451
	Co. Ar. [mm ²]:	0.8074 ± 0.0322	0.8068 ± 0.0339	-0.1	0.9696
	Co. Th. [mm]:	0.1840 ± 0.0054	0.1864 ± 0.0065	+1.3	0.3830
6 Months	Indices	Ig	CTLA4-Ig	% Change	P
L3 Vertebrae	BV/TV [%]:	13.33 ± 1.05	16.91 ± 1.76	+26.9	*0.0001
	Tb.Th. [mm]:	0.0450 ± 0.0027	0.0474 ± 0.0026	+5.3	*0.0447
	Tb.N. [/mm]:	3.15 ± 0.12	3.53 ± 0.31	+12.1	*0.0001
	Tb. Sp. [mm]:	0.3195 ± 0.0155	0.2843 ± 0.0222	-11.0	*0.0002
Femur	BV/TV [%]:	3.24 ± 1.01	4.42 ± 1.32	+36.6	*0.0262
	Tb.Th. [mm]:	0.0442 ± 0.0045	0.0485 ± 0.0060	+9.7	0.0631
	Tb.N. [/mm]:	2.67 ± 0.19	2.76 ± 0.16	+3.4	0.2349
	Tb. Sp. [mm]:	0.3791 ± 0.0273	0.3666 ± 0.0243	-3.3	0.2640
	Co. Ar. [mm ²]:	0.7462 ± 0.0268	0.7835 ± 0.0597	+5.0	0.0630
Co. Th. [mm]:	0.1898 ± 0.0072	0.2000 ± 0.0104	+5.4	*0.0114	

Mean ± SD; 3 mo. N=10 mice/group; 6 mo. n= 12 Ig and 11 CTLA4-Ig mice/group; Exact P values, *p<0.05.

Table II

μ CT Indices from Mature Mice administered Ig or CTLA4-Ig for 6 months

Mature Mice	Indices	Ig	CTLA4-Ig	% Change	P
L3 Vertebrae	BV/TV [%]:	11.74 \pm 1.26	13.31 \pm 1.85	+13.4	0.0730
	Tb.Th. [mm]:	0.0508 \pm 0.0034	0.0492 \pm 0.0045	-3.2	0.4324
	Tb.N. [/mm]:	2.72 \pm 0.12	2.94 \pm 0.19	+8.2	*0.0154
	Tb.Sp. [mm]:	0.3658 \pm 0.0170	0.3409 \pm 0.0222	-6.8	*0.0292
Femur	BV/TV [%]:	0.82 \pm 0.48	1.11 \pm 0.67	+36.1	0.3275
	Tb.Th. [mm]:	0.0506 \pm 0.0111	0.0406 \pm 0.0128	-19.7	0.1181
	Tb.N. [/mm]:	2.35 \pm 0.14	2.39 \pm 0.21	+1.7	0.6608
	Tb.Sp. [mm]:	0.4197 \pm 0.1075	0.4463 \pm 0.0353	+6.3	0.5171
	Co.Ar. [mm ²]:	0.7716 \pm 0.0314	0.7940 \pm 0.0419	+2.9	0.2464
	Co.Th. [mm]:	0.1774 \pm 0.0085	0.1769 \pm 0.0135	-0.3	0.9306

Mean \pm SD; Mature Mice: n=8 Ig and 7 CTLA4-Ig mice/group. Exact P values are indicated and *p<0.05.

Table III

Histomorphometry of Femurs from Ig and CTLA4-Ig Injected Mice

Structural Indices	Ig	CTLA4-Ig	% Change	P
BV/TV [%]:	2.07 ± 0.83	3.96 ± 1.27	+91.4	*0.0004
BS [mm]:	2.40 ± 1.19	4.13 ± 1.14	+71.9	*0.0025
Tb.Th [mm]:	0.0277 ± 0.0037	0.0305 ± 0.0040	+10.2	0.1039
Tb.N [/mm]:	0.76 ± 0.32	1.28 ± 0.31	+68.9	*0.0010
Tb. Sp [mm]:	1.679 ± 1.167	0.812 ± 0.279	-51.6	*0.0333
Dynamic Bone Formation Indices				
MS [mm]:	1.42 ± 0.58	2.01 ± 0.736	+41.5	*0.0148
MS/BS [%] ^a :	42.59 ± 8.18	44.11 ± 7.00	+3.6	0.6486
MAR [µm/day]:	1.44 ± 0.25	1.62 ± 0.19	+13.0	*0.0443
BFR/BS [µm/day]:	0.607 ± 0.136	0.717 ± 0.151	+18.1	0.0870
BFR/TV [/day]:	0.0013 ± 0.0007	0.0020 ± 0.0007	+51.0	*0.0315
BFR/BV [/day]:	0.0394 ± 0.0087	0.0394 ± 0.0019	+0.2	0.9879
Osteoblast Indices				
ObS/BS:	26.98 ± 15.82	21.49 ± 9.74	-20.4	0.3555
N.Ob/BS:	14.02 ± 7.95	12.19 ± 5.60	-13.0	0.5478
Osteoclast Indices				
OcS/BS:	6.81 ± 3.12	5.35 ± 2.49	-21.5	0.2453
N.Oc/BS:	1.98 ± 0.78	1.89 ± 0.92	-4.6	0.8051

Mean ± SD; N=12 Ig and 10 CTLA4-Ig. Exact P values are indicated and *=p<0.05.

^aMS/BS [%] = (dLS+sLS/2)/BS*100